University of New Hampshire
University of New Hampshire Scholars' Repository

Earth Sciences Scholarship   Earth Sciences

1998

Characteristics of modern atmospheric dust deposition in snow on the Penny Ice Cap, Baffin Island, Arctic Canada

Christian Zdanowicz
University of New Hampshire, Durham

Gregory A. Zielinski
University of New Hampshire - Main Campus

Cameron P. Wake
University of New Hampshire - Main Campus, cameron.wake@unh.edu

Follow this and additional works at: https://scholars.unh.edu/earthsci_facpub

Characteristics of modern atmospheric dust deposition in snow on the Penny Ice Cap, Baffin Island, Arctic Canada

By C. M. ZDANOWICZ[1], G. A. ZIELINSKI and C. P. WAKE, *Climate Change Research Center, Institute for the Study of Earth, Oceans and Space, University of New Hampshire, Durham NH 03824, USA*

ABSTRACT

We evaluated the concentration, size and distribution of insoluble dust microparticles in snow-pits on the Penny Ice Cap (PIC), Baffin Island, to define (1) the characteristics of modern atmospheric dust deposition at the site, (2) the relative contributions of proximal and distal dust sources, and (3) the effects of summer melting on depositional signals in snow. The mean concentration (143 µg kg^{-1}), flux (4.8 µg cm^2 yr^{-1}) and diameter (2.3 µm) of dust deposited on the PIC are similar to those observed in remote Arctic sites such as central Greenland, implying that dust is primarily supplied through long-range transport from far-removed source regions (at least 10^2–10^3 km distant). There is evidence for two seasonal maxima of dust deposition, one in late winter-early spring and one in late summer-early fall, although seasonal signals can not always be resolved in the snowpack due to some post-depositional particle migration with summer melt. However, ice layers appear to limit the mobility of particles, thereby preserving valuable paleoclimatic information in the PIC ice core dust record at a multi-annual to decadal temporal resolution.

1. Introduction

Insoluble mineral microparticles deposited in polar snow originate primarily from wind deflation of soils and sediments over continental source regions (Murozumi et al., 1969; Kumai, 1977; Hinkley, 1992). Because atmospheric dust deposition on glaciers frequently follows a seasonal cycle, microparticles can be used to identify annual layering in ice cores, provided the depositional sequence is preserved in the stratigraphy (Hamilton and Langway, 1967; Hammer et al., 1978). Changes in the concentration and size distribution of ice core dust particles are also used to document past changes in the atmospheric dust load or the dynamics of airborne dust transport and deposition (Thompson and Mosley-

Thompson, 1981; Petit et al., 1981, 1990; Hansson, 1995; Zielinski and Mershon, 1997).

Accurate interpretation of ice core dust records requires an understanding of the various physical factors that affect the measured concentration, variability, and size distribution of dust in ice. Here we present results of an investigation on the deposition and post-depositional modification of dust microparticles in snow on the Penny Ice Cap (PIC; 67° N; 65° W), southern Baffin Island, Arctic Canada (Fig. 1). This study will assist in the interpretation of a continuous Holocene record of dust deposition currently being developed from a 334 m surface-to-bedrock ice core drilled in 1995 from the summit region of the PIC. The specific objectives of this investigation are to: (1) define the modern characteristics of dust deposition in snow on the PIC (flux, size distribution, input timing) in order to establish a basis for interpreting the ice core dust record, (2) evaluate the relative

---

[1] Corresponding author.
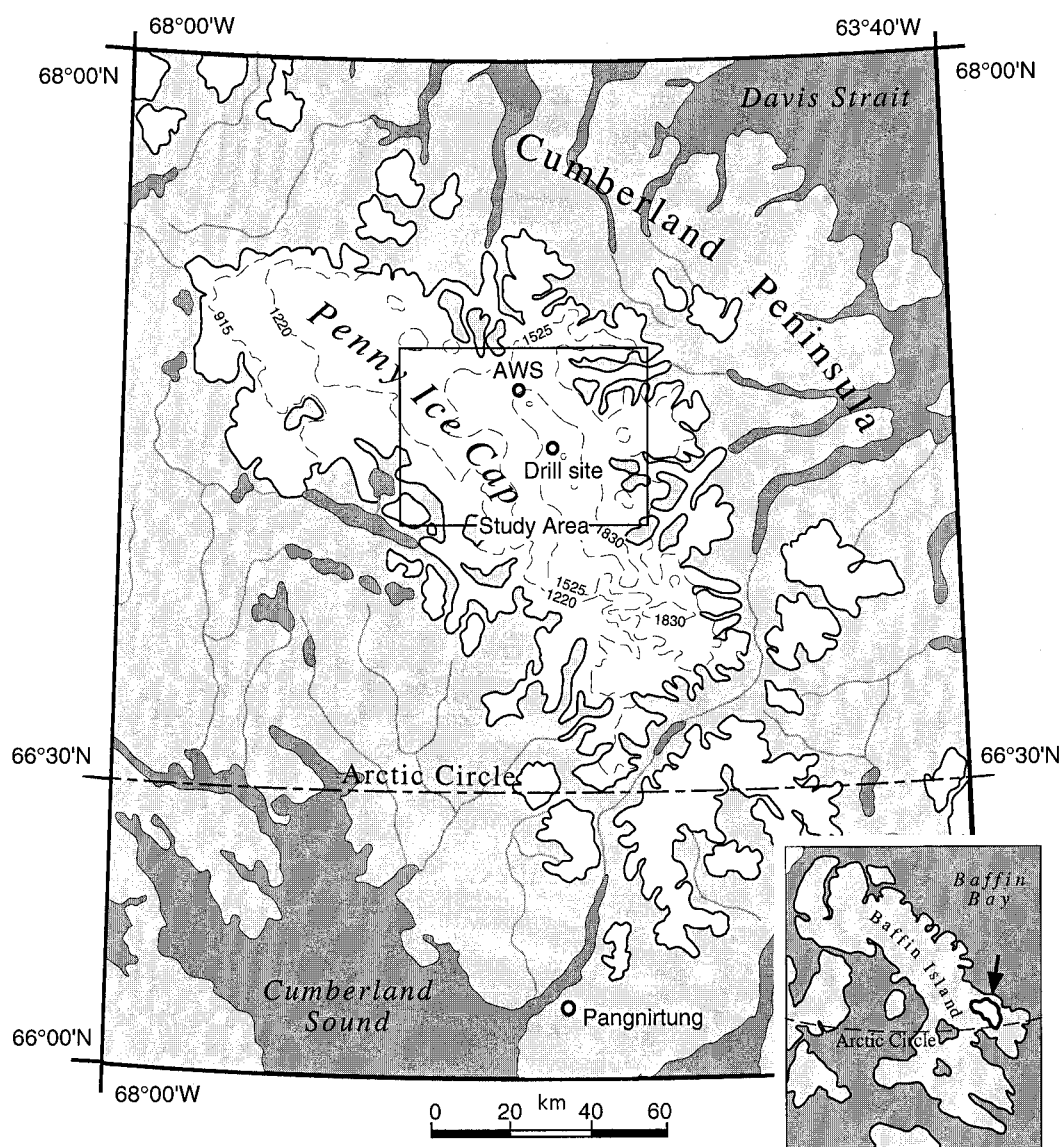e-mail: cmz@christa.unh.edu

Fig. 1. Location map of the Penny Ice Cap, Cumberland Peninsula, southern Baffin Island. The location of the automatic weather station (AWS) and ice core drilling site are shown. Contour intervals in meters.

contribution of proximal and distal sources to dust deposition on the PIC, and (3) evaluate the effects of summer melting on the preservation of dust depositional signals in the ice.

Previous investigations showed the potential for long-range eolian transport of mineral dust to the Arctic, including possible dominant source regions and transport pathways. The transport of

Eurasian dust plumes over Alaska was extensively discussed by Shaw (1980) and by Rahn et al. (1981). Welch et al. (1991) described a major dust fallout event over the Keewatin region which they attributed to an Asian source on the basis of composition and air-mass trajectories. Mullen et al. (1972), Darby et al. (1974) and Rahn et al. (1979) presented various estimates of the atmo-

spheric dust flux to the Arctic Ocean. Studies pertaining to the transport and deposition of dust to Greenland may be found in (among others) special journal issues on the Dye 3 Aerosol and Gas Sampling Program (*Atmos. Env.* **27A**, no. 17/18, 1993) and the Greenland deep ice cores (*J. Geophys. Res.* **102**, no. C12, 1997). However to the best of our knowledge, the only study of dust deposition to the Canadian ice caps previously published is that of Koerner (1977), who examined the distribution of microparticles $> 1 \mu m$ in snowpits and ice cores from the Devon Island Ice Cap. We later compare his findings with ours.

2. Methods

In April-May 1994 and 1995, a total of 6 snowpits, ranging in depth from 1.70 to 5.15 m, were excavated within a 10 km^2 area on the summit region of the PIC (~ 1980 m asl; Fig. 1) as part of a survey of snow stratigraphy and chemistry. Surface snow samples were also collected on a daily basis during the 1995 field season. Snowpits 94-1 and 95-4 were dug near a permanent automatic weather station (AWS) maintained by Canada's Atmospheric Environment Service, thus allowing us to compare snowpit stratigraphy with snow depth soundings and daily temperature readings (Grumet et al., 1998). Snowpit walls were sampled at 3 to 5 cm resolution by personnel wearing non-particulating clean suits, masks and gloves and using pre-cleaned polyethylene tools and containers. Although the mean annual surface temperature at the summit of the PIC is about $-16°C$, the study area is affected by summer melting and refreezing, leading to the formation of ice layers in the snowpack. Based on visual analysis of ice core stratigraphy, the average annual percentage of melt was estimated at about 50% (mass) for the last 100 years (R. M. Koerner, personal communication). Average accumulation rate for the period 1963–1995 was estimated to be 0.38 m ice equivalent (i.e.) using the beta-radioactive 1963 bomb fallout reference horizon in the ice core.

All snowpit and surface snow samples were shipped frozen from the PIC and stored at $-15°C$ until prior to analysis. Samples were then melted and aliquots were collected for microparticle and chemical analyses. Microparticle concentrations and size distributions were measured on an Elzone™ 280PC particle counter equipped with a 30 μm orifice. Measurements were performed under class 100 conditions on sample aliquots diluted with a prefiltered NaCl solution to give a 2% vol. electrolyte concentration. The particle counter was calibrated with monodisperse latex spheres with diameters of 1 and 5 μm. The data were acquired for a size range of 0.65 to 12 μm equivalent spherical diameter (d) in 64 logarithmically-distributed size channels. Routine analysis of filtered deionized water blanks showed background counts to be on average 10 times lower than in samples. Consequently background counts were not substracted from the sample data. All samples were analyzed in random order and in triplicate. Results were then averaged for individual samples, yielding an estimated error of 10% or less on particle concentrations. Because some dust fraction composed of soluble mineral phases such as $CaCO_3$ and $CaSO_4$ may be lost to solution during analysis, some discrepancy may exist between the actual dust concentration in the snow and the measured concentrations.

Microparticle concentrations for $0.65 < d < 12 \mu m$ are reported here as total number of particles (N) per ml H_2O and in terms of mass (M) as $\mu g \text{ kg}^{-1}$ ice or ppb. The mass and volume size distribution of microparticles were calculated from the raw count data by assuming spherical particles of uniform density $\rho = 2.6 \text{ g cm}^{-3}$, which is close to that of average crustal material. M was derived by integrating the mass size distribution over the measured diameter range and normalizing the result to the sample volume. This calculation may slightly underestimate the actual mass concentration, as it does not account for the contribution of particles with $d > 12 \mu m$. However, the infrequent obstruction of the 30 μm particle counter inlet indicated that coarse particles are rare. For each of our samples we calculated the number mean diameter (NMD) which represents the weighted arithmetic average of the number size distribution. Note that while NMD is a convenient parameter for quantifying relative changes in particle size, it may not represent the true mode of the number size distribution over the measured size range. We also computed the slope β of the log-linear Junge distribution

$$\ln \left[\frac{dN}{d(\ln d)} \right] = -\beta \ln d + \ln C,$$

fitted to particles with $d < 5\,\mu m$ (Junge, 1963). The coefficient β is inversely related to the coarseness of the microparticle population and can therefore be used to characterize it (Steffensen, 1985). For example, a higher value of β may imply relatively more fine particles and/or fewer coarse particles in the size distribution, and inversely for low β values.

In addition to microparticles, the concentration of eight major ions (Na^+, NH_4^+, K^+, Mg^{2+}, Ca^{2+}, Cl^-, NO_3^- and SO_4^{2-}) were measured at trace levels on a Dionex™ 4000i ion chromatograph using the procedure described in Buck et al. (1992). Duplicate analyses on 10% of all samples yielded a precision of 8% for K^+ and less than 5% for all other species. In addition to microparticles and ionic chemistry, sample aliquots from snowpit 94-1 were analyzed for oxygen isotopes at the Department of Geophysics of the University of Copenhagen. Results are expressed as $\delta^{18}O$ (‰) normalized to SMOW.

3. Results and discussion

3.1. Dust concentration and flux

To determine how representative dust deposition on the PIC is of regional to hemispheric atmospheric fallout, we compared the mean PIC dust concentration and flux with similar measurements from remote polar and non-polar sites (Table 1). The mean concentration of microparticles with $0.65\,\mu m < d < 12\,\mu m$ in the PIC snowpack is $31.6\ (\pm 19.4) \times 10^3\,ml^{-1}$ with a mass concentration of 143 (± 84) $\mu g\,kg^{-1}$. For particles with $d > 1\,\mu m$, the mean concentration is of 13.7 ($\pm 8.5) \times 10^3\,ml^{-1}$, which is comparable to that measured on the Devon and Agassiz ice caps and in central Greenland. Based on the estimated accumulation rate of 0.38 m ice yr^{-1}, we derived an average value for the modern eolian dust flux to the PIC of 4.8 $\mu g\,cm^{-2}\,yr^{-1}$ for particles with $0.65\,\mu m < d < 12\,\mu m$, and 4.4 $\mu g\,cm^{-2}\,yr^{-1}$ for particles with $d > 1\,\mu m$. This last value agrees closely with a 7000-year average value of 4.2 $\mu g\,cm^{-2}\,yr^{-1}$ for the Devon Ice Cap and falls within the range of 1 to 21 $\mu g\,cm^{-2}\,yr^{-1}$ obtained from various sites throughout the Arctic region. However, one must be aware that the values in Table 1 were obtained by several different methods

(see table caption), each entailing certain limitations. For example, mass calculations based on particle counter data may vary depending on the size range of particles measured, and on their assumed density. Similarly, dust concentrations derived from chemical data can vary depending on which element (Al, Si, Ca, Mn, etc.) is measured and its assumed abundance in crustal dust. Nevertheless, Table 1 shows the depositional flux of dust to the PIC to be essentially similar to that observed at various remote sites throughout the Northern Hemisphere. This suggests that dust deposition on the PIC is representative of the background crustal aerosol on a regional ($10^3\,km^2$) or larger scale.

3.2. Size distribution of dust and source proximity

In order to assess further the relative contribution of proximal and distal sources to the PIC snowpack, we determined the microparticle size distribution characteristics of our snowpit samples. For this, we applied a least squares regression to fit the measured particle volume distributions with a log-normal curve of the form

$$\frac{dV}{d\ln d} = \frac{V}{\sqrt{2\pi}\ln \sigma_g} \exp\left[-\frac{\ln^2(d/d_v)}{2\ln^2 \sigma_g} \right],$$

where V is the total particle volume over the size interval considered, d_v is the mode of the distribution and σ_g, the standard deviation. This type of distribution was previously found to provide a convenient representation of soil-derived aerosols and ice core microparticles (Patterson and Gillette, 1977; Wagenbach and Geiss, 1989; Steffensen, 1997). Because of the larger scatter of data at the upper and lower ends of the measured size range, we restricted the log-normal fit to a diameter interval of 0.8 to 5 μm. An example of microparticle size distribution fitted with a log-normal curve is shown on Fig. 2. Goodness of fit estimates for the log-normal model were obtained by the χ^2 method (Table 2). Consistently low (<1) values of χ^2 indicate that the log-normal model is a satisfactory approximation of the particle size distribution over the diameter range 0.8 to 5 μm.

Based on all snowpit samples ($n = 452$), we found the average volume size distribution of dust particles in the PIC snowpack to be centered around a mode of $2.3 \pm 2.1\,\mu m$. This value also represents the modal mass diameter d_m, since the

Table 1. *Atmospheric dust concentration and flux in snow and ice at various Northern Hemisphere sites*

	Site				Dust concentration and flux					
	lat	long	elevation (m asl)	Period[a] (years AD)	analytical method[b]	size range (μm)	number (10^3 ml^{-1})	mass (μg kg^{-1})	flux[c] (μg cm^{-2} yr^{-1})	Ref.
Canadian Arctic										
Penny Ice Cap	67° N	65° W	1980	1988–1994	CC	0.65–12	31.6	143	4.8	this work
					CC	1–12	13.7	129	4.4	
Agassiz Ice Cap	81° N	73° W	1600	1950–1977	CC	>1	18.3	n/a	n/a	Koerner and Fisher
				last 5000 years	CC	>1	18.2	n/a	n/a	(1982)
Devon Ice Cap	77° N	82° W	1800	last 7000 years	CC	>1	8.30	235	4.2	Fisher and Koerner (1981)
Arctic Ocean										
Canada basin	75° N	150° W	sea level	recent snow	FLTR	n/a	n/a	n/a	1.4 to 13.3	Darby et al. (1974)
Canada basin	84° N	72° W	sea level	recent snow	FLTR	n/a	n/a	n/a	8.5 to 21.0	Mullen et al. (1972)
Arctic ocean (average)			sea level	recent snow	CHEM	n/a	n/a	n/a	3.1	Rahn et al. (1979)
Greenland										
Summit	72° N	38° W	3207	recent snow	CC	0.5–12	n/a	46	1.0	Steffensen (1997)
Dye 3	65° N	43° W	2479	last 10 000 years	LLS	0.2–4	n/a	50	2.5	Hammer et al. (1985)
				1978–1983	LLS	0.2–4	9.4	n/a	n/a	
				1780–1951	LLS	0.2–4	20.0	n/a	n/a	
Camp Century	77° N	61° W	1885	recent snow	CHEM	n/a	n/a	35	1.4	Murozumi et al. (1969)
				1753–1965	EM	0.02–8	n/a	35	1.4	Kumai (1977)
sites A and D (average)	70° N	39° W	3070	1891–1910	LLS	0.2–4	n/a	74	2.5	Steffensen (1988)
inland sites (average)			>2400	1940–1950	LLS	>1	14.0	n/a	n/a	Hammer (1977)
Other sites										
Alaska range (USA)	63° N	151° W	2500	recent snow	CHEM	n/a	n/a	300	n/a	Hinkley (1994)
St-Elias range (USA)	60° N	139° W	2600	recent snow	FLTR	n/a	n/a	n/a	16.0	Windom (1969)
Mount Olympus (USA)	47° N	123° W	2000	recent snow	FLTR	n/a	n/a	n/a	32.0	Windom (1969)
Mont Blanc (France)	45° N	6° E	4270	1955–1985	CHEM	n/a	n/a	n/a	21.0 to 35.0	De Angelis and Gaudichet (1991)
Colle Gnifetti (Switzerland)	46° N	7° E	4450	1936–1982	CC	0.63–16	37.0	n/a	n/a	Wagenbach and
					CHEM	n/a	n/a	n/a	20.0	Geiss (1989)
Mustagh Ata (China)	38° N	75° W	5910	1990–1992	CC	1–22	276.4	6780	247	Wake et al. (1994)
Ngozumpa glacier (Nepal)	28° N	86° W	5700	1989–1990	CC	1–13	18.17	379	27	Wake et al. (1994)
Chongce ice cap (China)	35° N	81° W	6327	1980–1987	CC	1–22	616.0	8220	607	Wake et al. (1994)

[a] Period of snow accumulation represented by the data.

[b] Analytical methods: CC, Coulter counter or equivalent method; CHEM, calculated from chemical data (typically [Al], [Ca] or [Si]); EM, electron microscope; FLTR, based on dry filter weights; LLS, laser light scattering.

[c] Flux values were taken from the literature or calculated from mass concentrations using published estimates of snow accumulation rates.
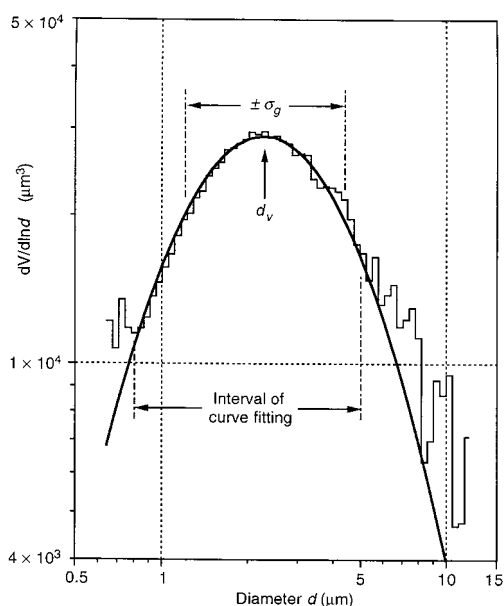
Fig. 2. Example of a log-normal curve fitted to micro-particle volume distribution data. The histogram is a stacked average of 30 snowpit samples. The size interval 0.8 to 5 μm over which curve fitting was applied is indicated. Mode (d_v) and standard deviation (σ_g) of the modeled distribution are also defined.

volume and mass size distributions are linearly related by $M(d) = \rho V(d)$ where ρ is the particle density. Other modes may exist for $d < 0.65$ μm, but there probably are none for $d > 12$ μm since particles of that size are rare. When compared to

measurements from other polar and non-polar sites (Table 3), the size mode of dust deposited on the PIC is found to be similar to that at Summit, central Greenland $(1.7 \pm 2.0$ μm). In view of the remoteness of Summit from continental dust sources, this suggests that atmospheric dust is delivered to the PIC by long-range transport from source regions distant by hundreds to thousands of km. Because coarse airborne particles settle out rapidly, the size distribution of dust aerosols shifts to an increasingly finer mode during long-range transport, such that beyond distances of several thousands of km the modal diameter approaches 1 μm (Radke et al., 1980; Schütz et al., 1981). A far-removed origin for the PIC dust is also supported by comparison with the mid-latitude, high elevation sites listed in Table 3. Mustagh Ata and the Chongce Ice Cap are located near the Taklamakan desert of central Asia and are characterized by rates of dust deposition in excess of 200 μg cm^{-2} yr^{-1} (Wake et al., 1994), which accounts for the coarser mode of dust measured in snow at these sites (3.7 μm $< d_v <$ 5.7 μm). Colle Gnifetti (Swiss Alps), although distant from North Africa by 1000 km, experiences Saharan dust fallout that can raise the concentration in snow up to 200 times above its baseline value of 20 μg cm^{-2} yr^{-1}. In this case, the rapid transit time of Saharan dust across the Mediterranean Sea accounts for its coarse mode $(d_v = 4.5$ μm) despite the long transport distance. In contrast, background dust deposited between Saharan dust

Table 2. *Concentration and volume size distribution*[a] *of dust in Penny Ice Cap snowpit samples based on (a) stratigraphy and (b) inferred timing of deposition*

Distribution	n	M(μg kg^{-1})	V (ppbv)	d_v (μm)	σ_g (μm)	r^2	χ^2
(a) snow	117	169.6	64.0	2.2 ($\pm$0.9)	2.1 ($\pm$1.4)	0.99	0.07
firn	251	138.9	52.4	2.3 ($\pm$1.0)	2.1 ($\pm$1.4)	0.99	0.06
hoar	39	78.2	29.5	2.0 ($\pm$1.0)	2.3 ($\pm$2.5)	0.90	0.32
ice	45	150.5	56.8	2.4 ($\pm$1.4)	2.3 ($\pm$1.9)	0.98	0.18
(b) winter	24	144.7	54.6	2.0 ($\pm$0.5)	1.9 ($\pm$0.9)	0.95	0.57
fall	28	193.2	72.9	2.9 ($\pm$2.3)	2.4 ($\pm$2.2)	0.98	0.42
spring + summer	42	144.2	54.4	2.2 ($\pm$1.0)	2.1 ($\pm$1.3)	0.99	0.16
all samples	452	143.1	54.0	2.3 ($\pm$1.1)	2.1 ($\pm$1.6)	0.99	0.03

[a] The cumulative volume (V), mode (d_v) and standard deviation (σ_g) of the size distributions were calculated by a log-normal curve fitting procedure as described in text. The log-normal distributions are plotted on Fig. 4. n is the number of samples per sample category. Errors on d_v and σ_g are shown in parentheses. Goodness of fit estimates $(r^2$ and $\chi^2)$ are given for n-4 degrees of freedom.

Table 3. *Size distribution characteristics of microparticles and mineral aerosols measured at various sites in the Northern Hemisphere*

	Size distribution parameters[a]			Dust source(s) and transport distance[b]	Ref.
	range (μm)	d_v (μm)	σ_g (μm)		
(a) Microparticles (modern snow)					
Penny Ice Cap, Canada	0.8 to 5	2.3	2.1	background, (local)	this work
Summit, Greenland	0.4 to 2	1.7	2.0	background	Steffensen (1997)
Colle Gnifetti, Switzerland	0.63 to 16	4.5	2.2	N. Africa; ⩾1000 km	Wagenbach and Geiss (1989)
	0.63 to 16	2.5	1.9	background, (local)	
Mustagh Ata, China	0.98 to 22	5.7	2.1	central Asia; >100 km	Wake et al. (1994)
Chongce ice cap, China	0.98 to 22	3.7	2.0	central Asia; >100 km	Wake et al. (1994)
(b) Mineral aerosols[c]					
Sahara (Nigeria)	0.01 to 100	∼3		local dust	d'Almeida and Shütz (1983)
Sahara (Algeria)	0.1 to 20	∼3		local dust	Gomes et al. (1990)
Plains, Texas	0.3 to 20	4.6	2.1	local dust	Patterson and Gillette (1977)
Sal Island, Cape Verde	0.71 to 5.8	5.1	2.4	N. Africa; >500 km	Savoie and Prospero (1980)
Tudor Hill, Bermuda	0.52 to >16.8	2.4	3.4	N. Africa; >5000 km	Arimoto et al. (1997)
Ragged Point, Barbados	0.52 to >16.8	2.3	3.1	N. Africa; >5000 km	Arimoto et al. (1997)
Enewetak Atoll, N. Pacific Ocean	0.2 to 7	1.4 to 2.0		Asia; >5000 km	Duce et al. (1980)
Barrow, Alaska	0.025 to 8	∼2		Asia; 5000 km	Rahn et al. (1981)

[a] In most cases, the modal size (d_v) and standard deviation (σ_g) were calculated by fitting a log-normal curve to the sample volume or mass distribution over the particle diameter range considered.

[b] Background implies that sources are both multiple and remote by thousands of km, (local) implies minor local dust contributions.

[c] All aerosol data are from surface measurements, except for the Barrow aerosol which was collected at an altitude of ∼2 km. Note that some desert aerosols may display a coarse mode above 20 μm.

fallout episodes shows a modal size (d_v = 2.5 ± 1.9 μm) closer to that measured on the PIC and at Summit, Greenland.

To estimate the probable transport distance of atmospheric dust deposited on the PIC, we also compared the particle size distribution of our snowpit samples with those of soil-derived aerosol populations collected proximally and distally from known source regions (Table 3). Aerosol measurements from Texas and the Saharan region were made under conditions of moderate atmospheric dust loading. The Cape Verde, Barbados and Bermuda aerosols represent Saharan dust transported over the tropical Atlantic Ocean, while the Enewetak dust aerosol originated from the arid regions of central Asia. The Barrow data represent the mineral aerosol component of late winter Arctic haze layers sampled by aircraft over Alaska. Each of these aerosol populations is described by the log-normal mode and standard deviation of its volume or mass size distribution. However, because the aerosol data were gathered using different techniques (including nephelometers and cascade impactors), caution must be observed in drawing direct comparisons with ice core microparticle measurements. In particular, estimates of the size mode of aerosols based on cascade impactors measurements may entail considerable error due to particle bounce effects (Walsh et al., 1978) or to uncertainties inherent in the log-normal curve fitting procedure (Dzubay and Hasan, 1990). Keeping these limitations in mind, a comparison of values in Table 3 indicates that the size mode of microparticles deposited on the PIC is finer than that of soil-derived aerosols measured in arid, dust-producing regions such as northwest Africa, but closely resembles that of desert dust aerosols sampled thousands of km away from their sources. It is also noteworthy that the modal size of dust on the PIC approaches that of mineral aerosol transported over Barrow (Alaska) and attributed by Rahn et al. (1981) to long-range transport from the Gobi desert and/or Loess Plateau of China. Weekly aerosol observations at Alert (Ellesmere Island; 82.5° N) between 1980 and 1990 reveal that the spring peak concentration of soil-derived Al coincides with the maximum seasonal occurrence of dust storms in China (Barrie, 1995), thereby suggesting a long-range Asian source. A central Asian source has also been inferred for dust aerosols sampled in Keewatin, in the mainland Canadian Arctic (Welch et al., 1991). This does not rule out possible contributions from other remote sources (e.g. continental North America) or from more proximal dust sources near the PIC; however, this comparison further supports our conclusion that dust deposited in modern snow on the PIC is representative of the atmospheric dust fallout on a spatial scale of 10^3 km² or more.

3.3. Timing and variability of dust deposition

A comparison of dust concentration profiles from the 1994 and 1995 PIC snowpits (Fig. 3) reveals considerable variability between and within individual snowpits, making it difficult to identify correlative features among snowpit dust profiles. A two-factor analysis of variance of the 1995 snowpits revealed that for 1 to 2 years of snow accumulation, the variance of dust distribution within one snowpit is comparable to that among snowpits. Furthermore, the mean dust concentration does not differ significantly among snowpits, suggesting a relatively uniform dust fallout over a spatial scale of ⩽10 km². Grumet (1997) reported similar findings for the distribution of major ions in PIC snow. These results indicate that a record of dust or major ion deposition from a single snowpit site may be considered representative of deposition on the summit area of PIC when averaged over a period of a few years.

To define the seasonal timing of dust deposition on the PIC, we examined the distribution of microparticles in snowpits in relation to snowpack stratigraphy, δ^{18}O and major ion chemistry. For convenience, we chose to represent the distribution of major ions in the snowpack by profiles of Na$^+$ concentration (Fig. 3). Most of the other major ionic species measured (Cl$^-$, Ca^{2+}, Mg^{2+}, SO$_4^{2-}$ and NO$_3^-$) show very similar profiles (Grumet et al., 1998). Individual accumulation years were delineated in the snowpits by placing the end of the ablation season at the top of the icy firn and/or thick ice layers (Alt and Bourgeois, 1995). This interpretation is supported by the frequent occurrence above the ablation surface of depth hoar layers which generally form in late summer or fall when the air-snow temperature gradient is conducive to firnification (Alley et al., 1990; Paterson, 1993;
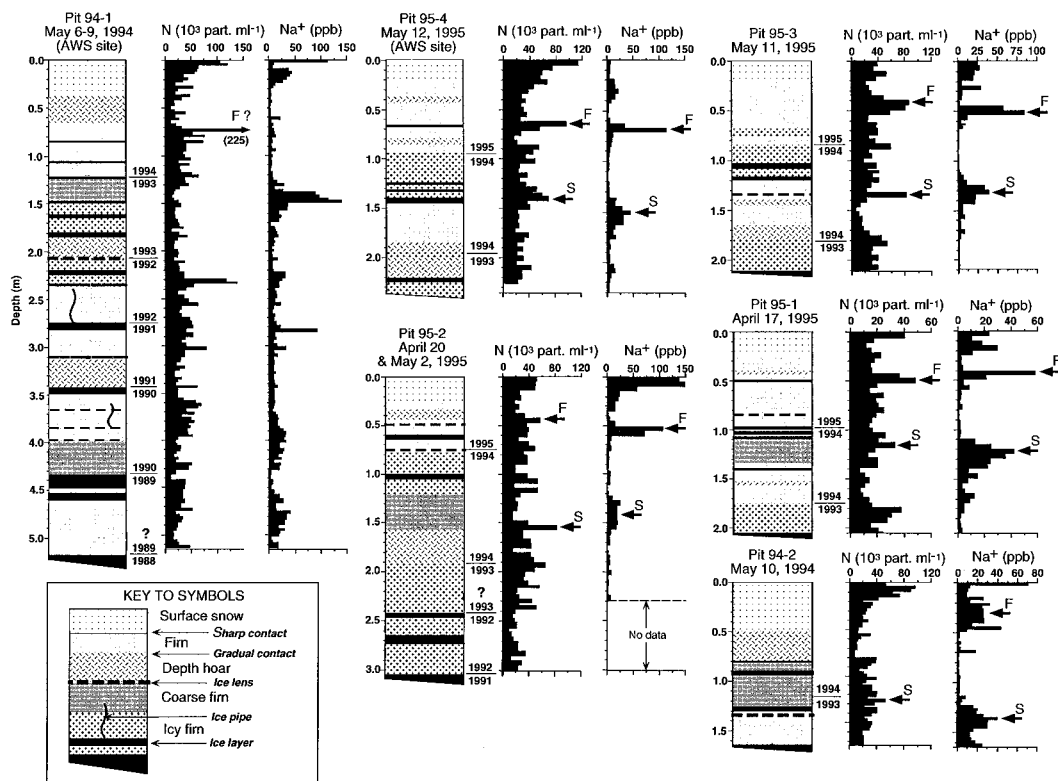
Fig. 3. Physical stratigraphy and profiles of dust (*N*) and Na⁺ concentration in six snowpits excavated at the summit of the Penny Ice Cap. Accumulation years are delineated by the end of the ablation season, as discussed in text. Arrows with labels indicate the inferred seasonal input timing for Na⁺ and dust peaks (S = Spring; F = Fall).

R. M. Koerner, personal communication). The presence of refrozen meltwater percolations and ice lenses in winter or fall firn layers indicates that summer meltwater can percolate and refreeze well below the ablation surface and into accumulation from previous years.

Comparison of the PIC snowpit profiles reveals the presence of two distinct dust concentration peaks in the upper part of all but one snowpit (i.e. pit 94-2). Based on our stratigraphic interpretation, we can assign the upper and lower peaks to late winter-spring and late summer-fall accumulation, respectively. The dust peaks also correlate approximately with distinct Na⁺ enhancements attributed by Grumet et al. (1998) to spring and fall depositional signals partly altered by meltwater redistribution during summer melt. These findings suggest that the PIC may experience two seasonal maxima of dust deposition. The lack of clear dust signals in the lower parts of most snowpits is attributed to post-depositional particle mobilization, as discussed later.

An explanation for the apparent bi-seasonal character of dust deposition on the PIC may be found by considering data from other polar sites. In the interior regions of Greenland and on the Devon Ice Cap, atmospheric dust deposition typically reaches a maximum in late winter or spring, although a second maxima in summer is not uncommon (Hamilton and Langway, 1967; Koerner, 1977; Hammer et al., 1978; Steffensen, 1985, 1988). Some arctic coastal sites surrounded by seasonally snow-free terrain also experience dust deposition in snow in late summer and/or early fall (Barrie and Barrie, 1990; Heidam et al., 1997). Thus, the seasonal doublet of dust concentration observed in the PIC snowpits may be

accounted for by contributions from both distal and possibly proximal (primarily in the fall and/or summer) sources. Furthermore, spring and fall are the dominant seasons of storm activity in the eastern Canadian Arctic, with the bulk of precipitation over southern Baffin Island supplied by cyclonic systems in the Baffin Bay-Davis Strait sector (Barry et al., 1973; Bradley and England, 1979; Keen, 1980). Thus, enhanced meridional flow and increased precipitation scavenging of atmospheric dust associated with spring and fall storm activity could contribute to an enhanced dust flux into snow in those seasons. However, some of the dust peaks seen in our PIC snowpit profiles may result from the concentration of dust by meltwater loss during melt episodes, as was observed on the Devon Ice Cap (Koerner, 1977) and at Dye 3, Greenland (Steffensen, 1985).

To better characterize dust deposited on the PIC under different meteorological regimes, we compared the size distribution of microparticles based on snowpit stratigraphy and on the inferred season of deposition. The mean particle size distributions for snow, firn, hoar and ice samples and for three seasonal intervals (fall, winter and spring + summer) were calculated by stacking the volume distribution data from individual samples. A weighted log-normal curve fit was then applied to the stacked distributions. We defined the seasonal intervals based on our stratigraphic interpretation of the 1995 snowpits, as discussed above. Because meltwater from summer ablation may cause displacement of particles below the uppermost melt layers, our calculations were restricted to the 1993–94 accumulation period for the 1994 snowpits, and to the 1994–95 period for the 1995 pits.

Results of these comparisons (Table 2, Fig. 4) indicate that on average, the concentration and modal size (d_v) of dust in fall accumulation are greater than for winter or spring + summer accumulation, although the size differences are within the error range. The coarser size of dust deposited with fall accumulation suggests a more important contribution from proximal dust sources at a time when snow cover extent is minimal. However the lack of very coarse particles and the overall fine mode of particles deposited in Penny Ice Cap snow indicate that such proximal sources are still relatively far from

the study site. By comparison, winter and spring + summer accumulation are nearly equal both in terms of dust concentration ($M \approx 144\ \mu g kg^{-1}$) and modal size ($d_v \approx 2\ \mu m$). This lack of difference suggests that the apparent late winter-spring deposition signal observed in our snowpit dust profiles primarily reflects the deposition of finer (submicron) particles transported from more distant sources. Our interpretation is in agreement with Steffensen's (1988) suggestion that microparticles deposited in Arctic spring snowfall may largely represent dust from distant sources that has accumulated in the Arctic troposphere during the winter season, when the extensive snow cover and southerly position of the polar front cut off more proximal dust sources. The data in Table 2 and Fig. 4 also show that the concentration of dust in hoar layers is significantly lower than in snow, firn or ice layers. This implies that maximum dust deposition in late summer-fall probably precedes the timing of depth hoar formation, as is suggested by the snowpit dust profiles.

3.4. Post-depositional redistribution of dust in the snowpack

Below the first summer melt layers, identification of seasonal dust signals in the PIC snowpits is ambiguous, with discrete peaks often lacking from the expected sequence. We attribute this primarily to post-depositional particle migration resulting from meltwater percolation during the ablation season. To investigate these post-depositional effects, we examined detailed depth profiles of microparticle parameters (N, NMD, β) and major ion chemistry (represented by Na^+) in snowpit 94-1, which spans the longest period of accumulation ($\geqslant 5$ years) of all our pits (Fig. 5). Our stratigraphic interpretation of pit 94-1 was found to be in overall good agreement with seasonal $\delta^{18}O$ excursions. However, we failed to identify any consistent relationship between dust concentration or size distribution, and ionic chemistry or snowpack stratigraphy. While some dust peaks are found to be associated with ice layers or Na^+ enhancements, others are not. Similarly, variations of NMD and β can not be systematically correlated to stratigraphic features of the snowpack. This lack of consistency indicates that microparticles are remobilized by meltwater in
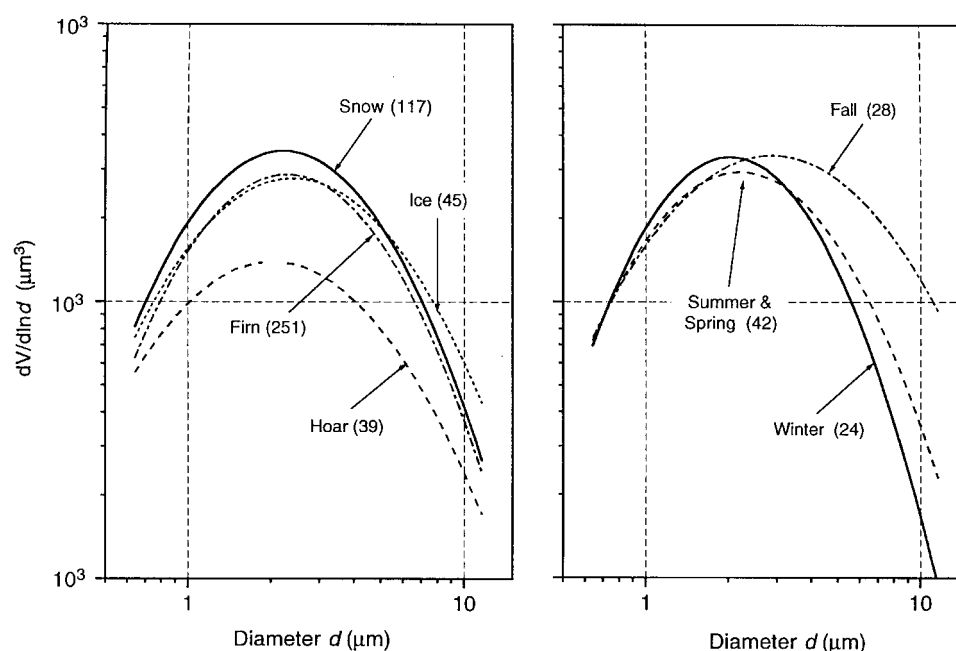
Fig. 4. Comparison of volume size distributions of microparticles in Penny Ice Cap snowpits based on stratigraphy (left) and on input timing (right). The volume size distributions were fitted with log-normal curves, the parameters of which are given in Table 2. Each curve represents an average of *n* samples, with *n* shown in parentheses on the curve labels.

such a way that seasonal (and stratigraphic) differences are obscured. At Dye 3, south Greenland, Steffensen (1985) observed that melt layers in a snowpit profile were generally correlated with low β values, suggesting preferential wash-out of the finer particles from the snow layers affected by melting. We observed no such relationship in snowpit 94-1, indicating that meltwater percolation in PIC snow affects both fine and coarse particles. However if meltwater was completely remobilizing dust particles in the snowpack, one would expect the resulting vertical distribution profiles to be flat. Instead, our snowpit dust profiles still display considerable structure and variability, as shown by baseline concentration variations of up to 10^4 ml^{-1} and by the presence of well-defined peaks. Factors that may preserve this variability are interannual variations of snow accumulation or summer melt. Another is the presence of numerous ice layers acting as physical obstacles against particle migration in snow, a scenario previously suggested by Grumet et al. (1998) for the translocation of major ions.

While we lack data to quantify the post-depositional migration of particles, we consider it unlikely that such migration would exceed a depth of 2–3 m in view of the frequency of ice layers in the snowpack. At the current rate of snow accumulation ($\sim$1 m yr^{-1}), a depth of 2–3 m would correspond to about 3 years of accumulation, which puts an approximate upper limit on the temporal resolution of our dust deposition record under present conditions. A higher resolution may be attainable in the ice core record during climatic periods that were characterized by lower summer melt %s than at present. To evaluate the preservation of dust variability over a longer interval of deposition, we performed a Fourier analysis on dust concentration against ice equivalent depth for the upper 20 m of the PIC core. Sampling resolution for this portion of the core was of 5 cm, which should be sufficient to resolve sub-annual variability of depositional signals if the latter are preserved. Results of our analysis reveal strong spectral power concentrated between 0.4 and 0.7 m ice eq., with a maximum (well above the 99.9%
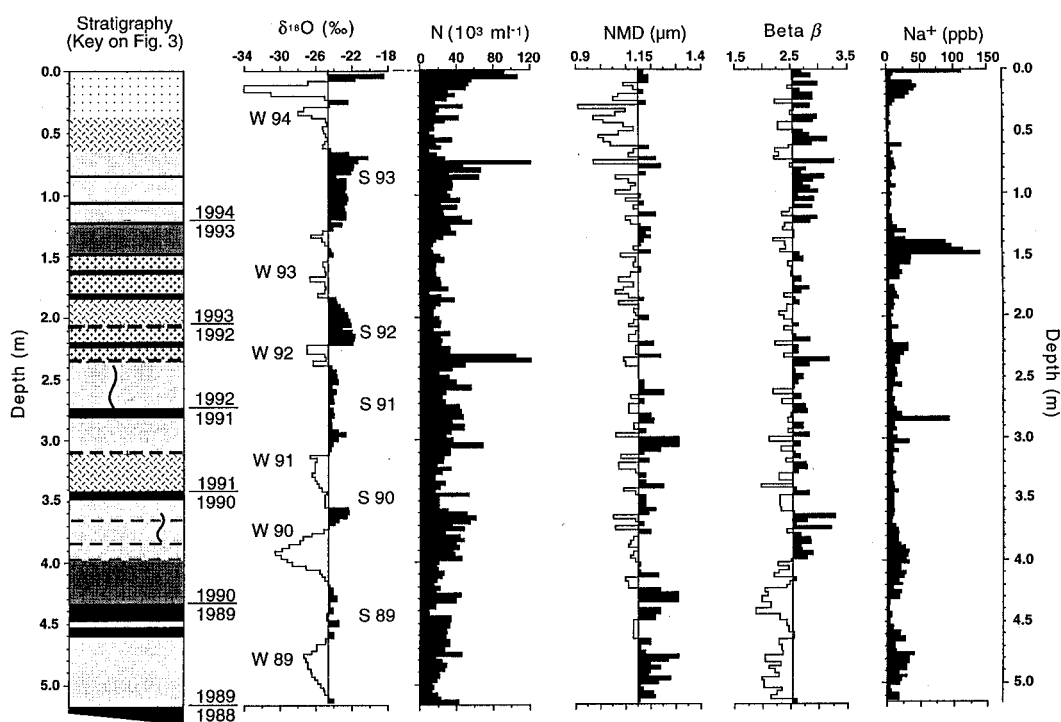
Fig. 5. Detailed stratigraphy and profiles of oxygen isotopes ($\delta^{18}O$), Na^+, dust concentration (N) and size distribution parameters (NMD, β) in snowpit 94-1. Stratigraphic symbols as defined on Fig. 3. Shading on the $\delta^{18}O$, NMD and β profiles highlight relative departure from the mean.
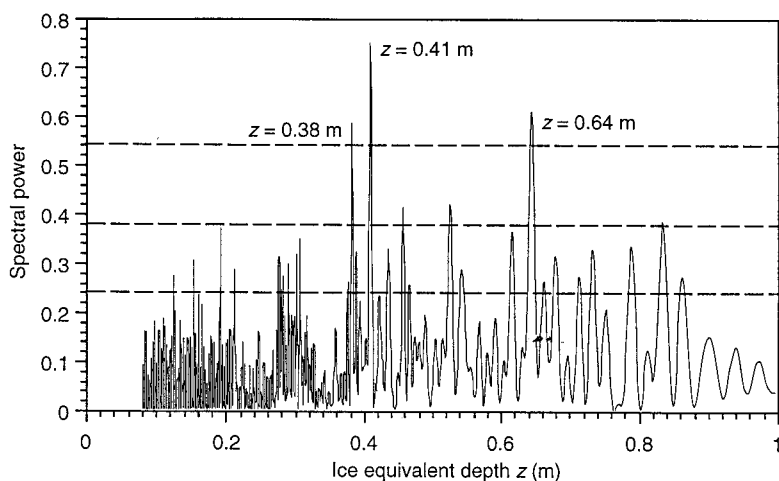

Fig. 6. Fourier power spectrum of microparticle concentrations (N) versus ice equivalent depth for the upper 20 m of the Penny Ice Core. The horizontal dashed lines represent (from top to bottom) the 99.9%, 99% and 95% confidence limits. Labels indicate the ice equivalent depth corresponding to peaks of maximum power density.

confidence level) at 0.41 m ice eq., remarkably close to our estimated modern annual accumulation rate of 0.38 m ice eq. (Fig. 6). These results do not imply that the original stratigraphic sequence of dust deposition is intact, but do support our contention that annual to multi-annual variability is still preserved downcore, as was previously shown for major ions (Grumet et al., 1998). Thus, valuable paleoclimatic information may still be obtained by considering multi-annual to decadal averages of the PIC ice core microparticle record.

4. Conclusions

Our analysis of dust distribution in snowpits on the PIC brings forth three main conclusions:

(1) The average concentration ($143 \, \mu g \, kg^{-1}$), flux ($4.8 \, \mu g \, cm^2 \, yr^{-1}$) and size mode ($2.3 \, \mu m$) of dust deposited in modern PIC snow are essentially similar to those observed in other remote Arctic sites such as central Greenland. Furthermore, the modal size of PIC dust ($d_v = 2.3 \, \mu m$) resembles that of desert dust aerosols transported over distances in excess of 1000 km. These similarities suggest that the bulk of dust deposited on the PIC originates from an atmospheric reservoir supplied through long-range transport of dust emitted from far-removed regions (i.e., 10^2 to 10^3 km distant).

(2) The variability of dust deposition in the PIC snowpack appears to be equal on a spatial scale of at least $10 \, km^2$ and a temporal scale of 1–2 years. There is some evidence for two seasonal maxima of atmospheric dust deposition, one in late winter-spring, one in late summer-fall, which correlate approximately with seasonal enhancements in major ion chemistry (Grumet et al., 1998). The slightly coarser mode ($\sim 3.0 \, \mu m$) of dust deposited with late summer-fall accumulation suggests some influence from more proximal (albeit still distant)

dust sources, possibly as a result of dust emissions from snow-free terrain in this time of the year. In contrast, the late winter-spring dust peak may primarily reflect the deposition of finer, far-traveled dust originating from sources such as continental North America or central Eurasia.

(3) Because of post-depositional particle migration, seasonal dust signals can not always be unambiguously resolved in the PIC snowpack. However the formation of ice layers limits the mobility of particles, such that redistribution is likely to be minimal beyond the depth equivalent of 3 years of snow accumulation. This is supported by the presence of strong yearly spectral component in the distribution of dust in the PIC ice core. These findings imply that while the Holocene dust record from the PIC core may not resolve inter-annual differences, it may still provide valuable paleoclimatic information at a multi-annual to decadal resolution.

5. Acknowledgements

REFERENCES

Alley, R. B., Saltzman, K. M., Cuffey, K. M. and Fitzpatrick, J. J. 1990. Summertime formation of depth hoar in central Greenland. *Geophys. Res. Lett.* **17**, 2393–2396.

Alt, B. T. and Bourgeois, J. C. 1995. Establishing the chronology of snow and pollen deposition events on Agassiz Ice Cap (Ellesmere Island, Northwest Territor-

ies) from autostation records. In: *Current Research 1995-B*, Geological Survey of Canada, Ottawa, 71–79.

Arimoto, R., Ray, B. J., Lewis, N. F., Tomza, U. and Duce, R. A. 1997. Mass-particle size distributions of atmospheric dust and the dry deposition of dust to the remote ocean. *J. Geophys. Res.* **102**, 15,867–15,974.

Barrie, L. A. 1995. Arctic aerosols: composition, sources

and transport. In: *Ice core studies of global biogeochemical cycles* (ed. R. J. Delmas). NATO ASI Series, Springer-Verlag, Berlin, 1–22.

Barrie, L. A. and Barrie, M. J. 1990. Chemical components of lower tropospheric aerosols in the High Arctic: six years of observations. *J. Atmos. Chem.* **11**, 211–226.

Barry, R. G., Bradley, R. S. and Jacobs, J. J. 1973. Synoptic climatological studies of the Baffin Island area. In: *Climate of the Arctic* (ed. G. Walker and S. Bowling). University of Alaska, Fairbanks, 82–90.

Bradley, R. S. and England, J. 1979. Synoptic climatology of the Canadian High Arctic. *Geog. Ann.* **61A**, 187–201.

Buck, C. F., Mayewski, P. A., Spencer, M. J., Whitlow, S. I., Twickler, M. S. and Barrett, D. 1992. Determination of major ions in snow and ice cores by ion chromatography. *J. Chrom.* **594**, 225–228.

d'Almeida, G. A. and Shütz, L. 1983. Number, mass and volume distributions of mineral aerosol and soils of the Sahara. *J. Clim. Appl. Meteorol.* **22**, 233–243.

Darby, D. A., Burckle, L. H. and Clark, D. L. 1974. Airborne dust on the Arctic ice pack, its composition and fallout rate. *Earth Planet. Sci. Lett.* **24**, 166–172.

De Angelis, M. and Gaudichet, A. 1991. Saharan dust deposition over Mont Blanc (French Alps) during the last 30 years. *Tellus* **43B**, 61–75.

Duce, R. A., Unni, C. K., Ray, B. J., Prospero, J. M. and Merrill, J. T. 1980. Long-range atmospheric transport of soil dust from Asia to the tropical North Pacific: temporal variability. *Science* **209**, 1522–1524.

Dzubay, T. G. and Hasan, H. 1990. Fitting multimodal lognormal size distributions to cascade impactor data. *Aerosol Sci. Tech.* **13**, 144–150.

Fisher, D. A. and Koerner, R. M. 1981. Some aspects of climatic change in the High Arctic during the Holocene as deduced from ice cores. In: *Quaternary paleoclimate* (ed. W. C. Mahaney). University of East Anglia Press, Norwich, 249–271.

Gomes, L., Bergametti, G., Coude-Gaussen, G. and Rognon, P. 1990. Submicron desert dust: a sandblasting process. *J. Geophys. Res.* **82**, 2074–2082.

Grumet, N. S. 1997. *Glaciochemical investigations of the last 1000 years from the Penny Ice Cap, Baffin Island.* MSc thesis, University of New Hampshire, Durham, NH, 90 pp.

Grumet, N. S., Wake, C. P., Zielinski, G. A., Fisher, D. A., Koerner, R. M. and Jacobs, J. D. 1998. Preservation of glaciochemical time-series in snow and ice from the Penny Ice Cap, Baffin Island. *Geophys. Res. Lett.* **25**, 357–360.

Hamilton, W. L. and Langway, C. C. Jr. 1967. A correlation of microparticle concentrations with oxygen isotope ratios in 700 year old Greenland ice. *Earth Planet. Sci. Lett.* **3**, 363–366.

Hammer, C. U. 1977. Dust studies on Greenland ice cores. In: *Isotopes and impurities in snow and ice.* International Association of Hydrological Sciences, Grenoble, 365–370.

Hammer, C. U., Clausen, H. B., Dansgaard, W., Gundestrup, N., Johnsen, S. J. and Reeh, N. 1978. Dating of Greenland ice cores by flow models, isotopes, volcanic debris and continental dust. *J. Glaciol.* **20**, 3–26.

Hammer, C. U., Clausen, H. B., Dansgaard, W., Neftel, A., Kristinsdottir, P. and Jonhson, E. 1985. Continuous impurity analysis along the Dye 3 deep core. In: *Greenland ice core: geophysics, geochemistry and the environment* (ed. C. C. Langway Jr., H. Oeschger and W. Dansgaard). American Geophysical Union, Geophysical Monograph 33, Washington, 90–94.

Hansson, M. E. 1995. Are changes in atmospheric cleansing responsible for observed variations of impurity concentrations in ice cores? *Ann. Glaciol.* **21**, 219–224.

Heidam, N. Z., Christensen, J., Wåhlin, P. and Skov, H. 1997. *Pollution of the Arctic troposphere: northeast Greenland 1990–1996.* National Environmental Research Institute, Roskilde, Denmark, 60 pp. – NERI Technical Report No. 221.

Hinkley, T. D. 1992. Variation of rock-forming metals in sub-annual increments of modern Greenland snow. *Atmos. Env.* **26A**, 2283–2293.

Hinkley, T. D. 1994. Composition and sources of atmospheric dust in snow at 3200 meters in the St. Elias Range, southeastern Alaska, USA. *Geochim. Cosmochim. Acta* **58**, 3245–3254.

Junge, C. E. 1963. *Air chemistry and radioactivity.* Academic Publishers, New York, 382 p.

Keen, R. A. 1980. *Temperature and circulation anomalies in the eastern Canadian arctic summer 1946–76.* Institute of Arctic and Alpine Research Occasional Paper No. 34, University of Colorado, Boulder, 159 p.

Koerner, R. M. 1977. Distribution of microparticles in a 299-m core through the Devon Island ice cap, Northwest Territories, Canada. In: *Isotopes and impurities in snow and ice.* International Association of Hydrological Sciences, Grenoble, 371–376.

Koerner, R. M. and Fisher, D. A. 1982. Acid snow in the Canadian High Arctic. *Nature* **295**, 137–140.

Kumai, M. 1977. Electron microscope analysis of aerosols in snow and deep ice cores from Greenland. In: *Isotopes and impurities in snow and ice.* International Association of Hydrological Sciences, Grenoble, 341–350.

Mullen, R. E., Darby, D. A. and Clark, D. L. 1972. Significance of atmospheric dust and ice rafting from Arctic Ocean sediment. *Geol. Soc. Amer. Bull.* **83**, 205–212.

Murozumi, M., Chow, T. J. and Patterson, C. 1969. Chemical concentrations of pollutant lead aerosols, terrestrial dusts and sea salts in Greenland and Antarctic snow strata. *Geochim. Cosmochim. Acta* **33**, 1247–1294.

Patterson, E. M. and Gillette, D. A. 1977. Commonalities in measured size distributions for aerosols having a soil-derived component. *J. Geophys. Res.* **82**, 2074–2082.

Paterson, W. B. 1993. *The physics of glaciers*, 3rd edition. Pergamon Press, Oxford, 480 p.

Petit, J. R., Briat, M. and Royer, A. 1981. Ice age aerosol

from East Antarctic ice core samples and past wind strength. *Nature* **293**, 391–394.

Petit, J. R., Mounier, L., Jouzel, J., Korotkevich, Y. S., Kotlyakov, V. I. and Lorius, C. 1990. Paleoclimatological and chronological implications of the Vostok core dust record. *Nature* **343**, 56–58.

Radke, L. F., Hobbs, P. V. and Eltgroth, M. W. 1980. Scavenging of aerosol particles by precipitation. *J. Appl. Meteor.* **19**, 715–722.

Rahn, K. A., Borys, R. D., Shaw, G. E., Schütz, L. and Jaenicke, R. 1979. Long-range impact of desert aerosol on atmospheric chemistry: two examples. In: *Saharan dust: mobilization, transport, deposition.* (ed. C. Morales). J. Wiley, New York, 243–266.

Rahn, K. A., Borys, R. D. and Shaw, G. E. 1981. Asian desert dust over Alaska: anatomy of an Arctic haze episode. In: *Desert dust: origin, characteristics, and effects on man* (ed. T. L. Péwé). *Geological Society of America Special Paper* **186**, 37–70.

Savoie, D. L. and Prospero, J. M. 1980. Water-soluble potassium, calcium, and magnesium in the aerosols over the tropical North Atlantic. *J. Geophys. Res.* **85**, 385–392.

Schütz, L., Jaenicke, L. and Pietrek, H. 1981. Saharan dust transport over the North Atlantic Ocean. In: *Desert dust: origin, characteristics, and effects on man* (ed. T. L. Péwé). Geological Society of America Special Paper **186**, 87–100.

Shaw, G. E. 1980. Transport of Asian desert aerosol to the Hawaiian Islands. *J. Appl. Meteor.* **19**, 1254–1259.

Steffensen, J. P. 1985. Microparticles in snow from the Greenland ice sheet. *Tellus* **37B**, 286–295.

Steffensen, J. P. 1988. Analysis of the seasonal variation in dust, Cl^-, NO_3^-, and SO_4^{2-} in two central Greenland firn cores. *Ann. Glaciol.* **10**, 171–177.

Steffensen, J. P. 1997. The size distribution of microparticles from selected segments of the Greenland Ice Core Project ice core representing different climatic periods. *J. Geophys. Res.* **102** (C12), 26,755–26,763.

Thompson, L. G. and Mosley-Thompson, E. 1981. Microparticle variations linked with climatic change: evidence from polar ice cores. *Science* **212**, 812–815.

Wagenbach, D. and and Geiss, K. 1989. The mineral record in a high altitude alpine glacier (Colle Gnifetti, Swiss Alps). In: *Paleoclimatology and paleometerology: modern and past patterns of global atmospheric transport* (ed. M. Leinen and M. Sarnthein). Kluwer Academic Publishers, Dordrecht, 543–564.

Wake, C. P., Mayewski, P. A., Li, Z., Han, J. and Qin, D. 1994. Modern eolian dust deposition in central Asia. *Tellus* **46B**, 220–233.

Walsh, P. R., Rahn, K. A. and Duce, R. A. 1978. Erroneous elemental mass-size functions from a high-volume cascade impactor. *Atmos. Env.* **12**, 1793–1795.

Welch, H. E., Muir, D. C. G., Billeck, B. N., Lockhart, W. L., Brunskill, G. J., Kling, H. J., Olson, M. P. and Lemoine, R. M. 1991. Brown snow: a long-range transport event in the Canadian Arctic. *Env. Sci. Tech.* **25**, 280–286.

Windom, H. L. 1969. Atmospheric dust records in permanent snowfields: implications to marine sedimentation. *Geol. Soc. Am. Bull.* **80**, 761–782.

Zielinski, G. A. and Mershon, G. R. 1997. Paleoenvironmental implications of the insoluble microparticle record in the GISP2 (Greenland) ice core during the rapidly changing climate of the Pleistocene-Holocene transition. *Geol. Soc. Am. Bull.* **109**, 547–559.